

# Semiconductor Optical Bistability and Switching

A. Sergio Bezerra Sombra

*Laboratório de Ótica Não Linear e Lasers, Departamento de Física  
Universidade Federal do Ceara, Campus do Pici, C. P. 6030, 60450 Fortaleza, CE, Brasil*

Received July 12, 1993; revised manuscript received September 17, 1993

Optical nonlinear switching and resonatorless bistability due to increasing absorption has been observed in a nondegenerate pump and probe experiment in Semiconductor (CdSSe) Doped Glass (YDG). With the proper choice of the parameters, like modulation frequency and light intensity, one hundred percent modulation in a probe laser induced by a strong pump laser was obtained at room temperature. Two nonlinear regimes were observed, with saturated pump absorption being dominant at high pump power.

## I. Introduction

Composite materials containing semiconductor microcrystallites show interesting possibilities for applications to all optical signal processing devices<sup>[1-3]</sup>. In particular, glasses doped with microcrystallites of  $\text{CdS}_x\text{Se}_{1-x}$  have been the subject of investigation because of their large nonlinearities ( $\chi^{(3)} \approx 10^{-8}$  esu at 532 nm<sup>[2]</sup>). Their properties are important in degenerate four wave mixing, optical phase conjugation<sup>[4,5]</sup> and bistability<sup>[3,6,7]</sup>.

Data on the non-linear optical properties of SDG have previously been obtained by means of pulsed nano to femtosecond lasers. For this reason some relatively slow relaxation processes in SDG have not been examined.

In this paper we describe a study of the non-linear properties of these glasses using a nondegenerate pump and probe technique. In this configuration probe modulation induced by a modulated pump is strongly dependent on pump intensity and modulation frequency.

## II. Experimental

The experimental setup is shown in figure 1. The 514,5 nm line of a CW argon ion laser (pump) and the 632.8 nm of a CW He-Ne laser (probe) were used. Pump and probe beams were focused into the sample using a lens of focal length 150mm resulting in a spot size of about 30  $\mu\text{m}$  of diameter. The pump beam was modulated with a chopper with a stability of about 1Hz

and able to operate at frequencies up to 4kHz. We used 2.8mm thick samples of corning glass (CS 2.63).

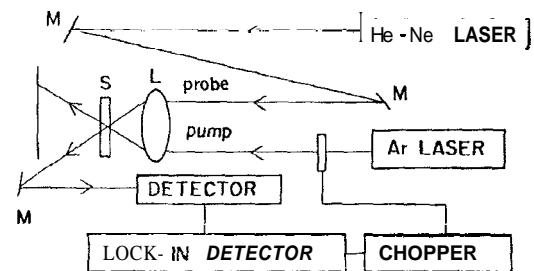


Figure 1: Experimental diagram for the study of optical properties in semiconductor doped glass using pump and probe technique.; M, mirror; L, lens; S, sample.

To measure the probe beam intensity and dephasing between pump and probe we employed a lock-in detector in conjunction with an oscilloscope.

All the intensity dependent results were obtained as the pump intensity was increased from zero to a maximum intensity  $I_0$  (or decreased), keeping the pump pulse duration constant. The time dependence of the probe beam intensity was observed collecting the probe beam after traversing the sample on a fast photodiode ( $\sim 0.1\mu\text{sec}$  response time) and feeding the signal to an oscilloscope.

## III. Results and discussion

In figure 2 we have the peculiarities of the probe transmission as a function of pump power. For pump powers greater than  $0.3I_0$  the probe beam is strongly

absorbed. For pump powers greater than  $0.5I_0$  the saturated absorption of the pump is dominant. From this point on the transmitted probe intensity starts increasing. Reducing the pump power, optical hysteresis is observed. We emphasize that the two distinct regions of switching are associated with optical bistability. In the first region ( $I_{pump} < I_0/2$ ) the reverse switching is a state of high absorption. In the second region the reverse switching is in a state of lower absorption. The first region is associated with the increasing absorption where in the second we have the normal bistability behaviour.

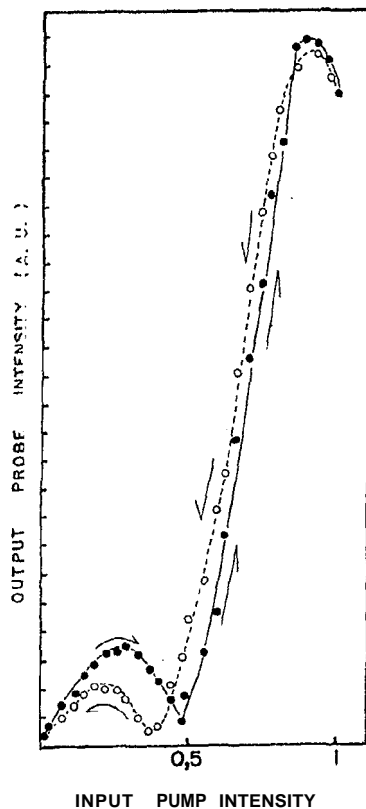


Figure 2: Bistability of the transmitted probe intensity vs input pump intensity. Horizontal scale  $I/I_0$ , ( $I_0 = 30\text{kW/cm}^2$ ),  $\tau_{\text{pump pulse}} = 10\text{ms}$  and  $T = 300\text{K}$ .

We show in figure 3 it the strong dependence of the dephasing between pump and probe with the pump intensity. The measured dephasing indicate different processes such as laser induced darkening (dephasing  $\approx -180^\circ$ ) or instantaneous laser induced clearing (dephasing  $\approx 0^\circ$ ). For intermediate pump values, between  $0^\circ$  and  $-180^\circ$  one has a delayed darkening. The transition from the clearing state to the darkening state occurs around  $\sim 0.5I_0$  and is very steep.

The variation of the probe signal intensity with

pump modulation frequency is shown in figure 4. Assuming an exponential decay one can reasonably fit the experimental data for probe intensity versus modulation frequency by a Lorentzian curve (Fourier transform). There is a good agreement for high frequencies. It is clear that the signal behaviour for low frequencies is much more complex than a simple exponential decay. Some experimental and theoretical work is in progress trying to explain this behaviour.

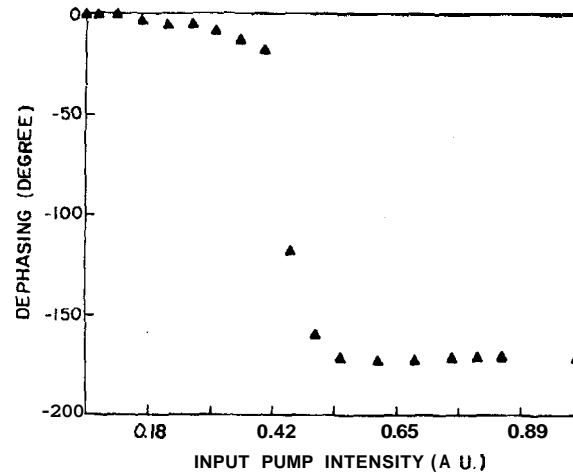


Figure 3: Dephasing between pump and probe pulses vs pump intensity (Horizontal scale is normalized,  $I/I_0$ , ( $I_0 = 30\text{kW/cm}^2$ )) with  $\tau_{\text{pump pulse}} = 10\text{ms}$ .

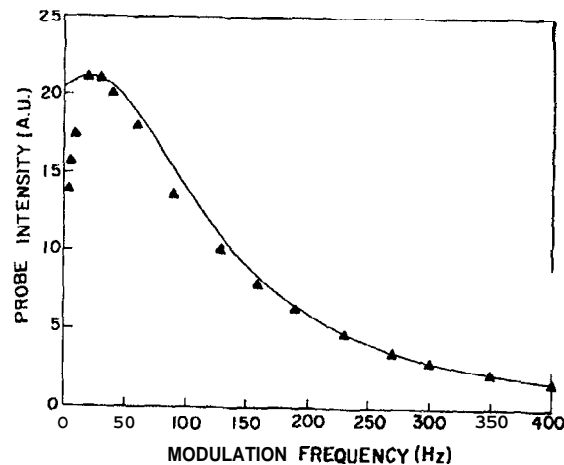


Figure 4: Probe intensity versus modulation frequency  $I_{\text{pump}} = 24\text{ kW/cm}^2$  with  $I(f) = I_{\text{max}} / (\tau^{-2} + (f - 21.1)^2)$ . Continuous line is  $I(f)$  with  $\tau = 8.9\text{ms}$  and  $I_{\text{max}} = 2.65 \cdot 10^5$  ( $f$  in Hz). (A) Experimental points.

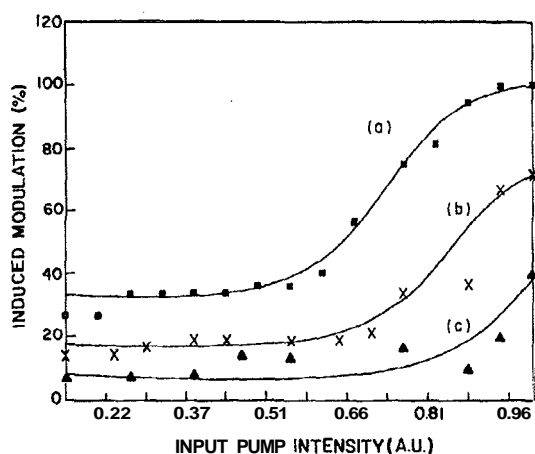


Figure 5: Induced probe modulation as a function of **pump** intensity (Horizontal scale is normalized,  $I/I_0=24\text{kW}/\text{cm}^2$ ), .a)  $f=50\text{Hz}$ , b)  $f=200\text{Hz}$ , c)  $f=400\text{Hz}$ . (Continuous line is a guide to the eye).

The relative modulation depth in the probe channel also increases with pump power (figure 5). The relative depth is maximum for high pump intensities and low

frequencies (Figure 5a). With the proper choices of parameters like pump intensity and frequency modulation one can have 100% modulation.

These results may be explained taking into account two major nonlinear mechanisms: during the input pulse the local temperature rises, the absorption edge shifts to the red and the probe thus beam spectrum falls into the region of high absorption. This behaviour is associated to the fact that in our experimental situation the wavelength of the probe pulse is close to the band edge ( $\lambda_{\text{gap}} \sim 630\text{ nm}$ ) and the pump laser has a large excess energy above the absorption edge of the SDG.

The transmission and reflection coefficients of the sample can be calculated taking into account the complex refractive index  $n = n + ik$  where  $k$  is related to the absorption coefficient by  $a = 4\pi k/\lambda_0$ . The transmittance and reflectance coefficients are respectively:

$$\tau(T) = (n_1(T)^2 e^{\alpha(T)d} + n_2(T)^2 e^{-\alpha(T)d} - 2n_1(T)n_2(T) \cos(2\delta(T)))^{-1}, \quad (1)$$

and

$$R(T) = \frac{n_2(T)n_1(T)(e^{\alpha(T)d} + e^{-\alpha(T)d} - 2 \cos(2\delta(T)))}{n_1(T)^2 e^{\alpha(T)d} + n_2(T)^2 e^{-\alpha(T)d} - 2n_1(T)n_2(T) \cos(2\delta(T))}, \quad (2)$$

with

$$n_1(T) = \frac{(n(T) + 1)^2}{4n(T)}, \quad n_2(T) = \frac{(n(T) - 1)^2}{4n(T)} \quad \text{and} \quad \delta(T) = \frac{2\pi n(T)d}{\lambda_0},$$

where  $d$  is the sample thickness,  $\lambda_0$  is the laser wavelength and  $\alpha$  is the absorption coefficient. In this case the absorption coefficient and the nonlinear index are temperature dependent.

Figure 6a. illustrates the behavior of the transmission function of the semiconductor doped glass give by  $T'(T) = 1 - \alpha(T)$ , where  $T$  is the sample temperature for a given probe wavelength. This temperature dependence of the absorption was used in eq. (1) for the calculation of the transmission coefficient. The strong nonlinearity of the absorption coefficient is associated to the fact that, for an increase of the pump power the temperature increases, the probe beam wavelength falls in the absorption band of the material and the absorption starts to increase (figure 6a). For very high pump intensities there is a saturated pump absorption which leads to an increase in the probe transmission (figure

6b). In figure 7 one can see a typical plot of the output probe intensity as a function of the input pump intensity calculated from eq. (1):  $P_t = \tau(T)P_i$ . In this simulation we took into account the dependence on temperature of  $\alpha$  (increasing absorption effect) (figure 6) and the temperature effect on the nonlinear index:  $n(T) = n_0 + \theta T$ , where  $n_0$  and  $\theta$  are positive constants. In this situation where  $a$  and  $n$  are temperature dependent one has both type of bistabilities (figure 7). For intensities around 0.17 one can see the switching for the high absorption state which is characteristic of the bistability of increasing absorption. If we increase the pump intensity there is another switching for a high transmission state which is the normal bistability behaviour. If we decrease the pump intensity both intensities of switching are present at low intensities but with large hysteresis. The behaviour of figure 7 occur for a

large variation of the parameters in eq. (1). One can use  $n_0$  in the range of 1.2 to 1.9 and  $\lambda_0$  in the visible region giving the same general behaviour. This simulation should be compared with experimental results in figure 2 where both bistabilities are present.

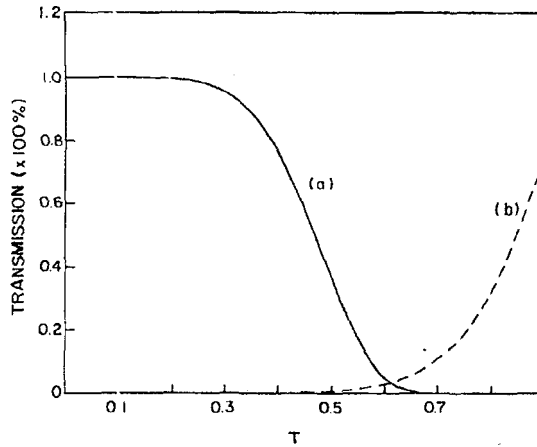


Figure 6: Probe transmission coefficient (%) as a function of temperature? (see text), a) increasing absorption, b) pump saturated absorption.

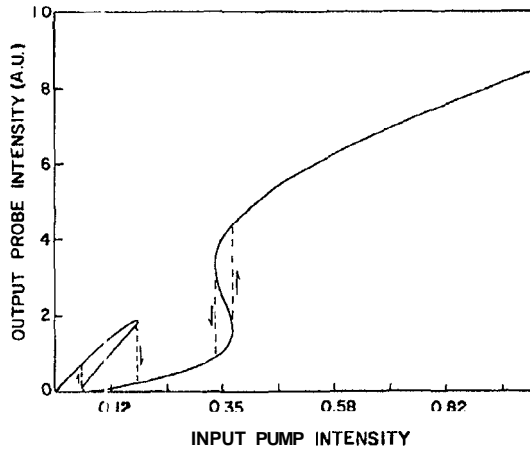


Figure 7: Simulation of the bistability of the transmitted probe intensity vs input pump intensity ( $n_0 = n = 1.6$  and  $\theta = 1/3 K^{-1}$  in normalized units used in figure 6).

The other effect that is also present, is the heat conduction through the sample according to the temperature transport equation (9):

$$\frac{\partial T}{\partial t} = \frac{I_0 A(T)}{C d \rho} - \frac{T - T_f}{\tau_T}, \quad (3)$$

where we assume a uniform intensity profile across the longitudinal dimension of the sample.  $I_0$  is the laser intensity,  $T_f$  is the surrounding temperature,  $\rho$  is the density,  $C$  is the specific heat,  $I_0 A(T)$  is the energy dissipated per unit of time and unit area with<sup>[8,9]</sup>,  $A(T) = 1 - R(T) - \tau(T)$  and  $d$  is the sample thickness. Taking in account that  $R \gg r_0$ <sup>[8]</sup>, we obtain

$$\tau_T = \frac{r_0^2}{4D} (1 + 2 \ln(R/r_0)) \quad \text{with} \quad D = \frac{K}{\rho C}. \quad (4)$$

Here  $R$  is the whole sample radius,  $2r_0$  is the minimum laser spot diameter,  $\rho$  is the density,  $K$  is the thermal conduction coefficient,  $D$  is the heat diffusion constant and  $\tau_T$  is the transverse relaxation time.

The relaxation time can be calculated from eq. (4) assuming  $r_0 = 15 \cdot 10^{-4}$  cm,  $R = 0.7$  cm,  $D = 3.8 \times 10^{-3}$  cm<sup>2</sup> s<sup>-1</sup>,  $K = 1.02 \times 10^{-2}$  W/cmK,  $\rho = 2.5$  g/cm<sup>3</sup> and  $C = 1.05$  J/gK. We have obtained  $\tau_T = 2$ ms while for our samples the measured switching time is around 3ms.

From these results one may conclude that for low frequencies ( $f = 50$ Hz,  $\tau_{\text{pump}} \sim 10$ ms  $\gg \tau_T$ ) and high pump powers the thermal effects dominates, leading to deep modulation (figure 5) and maximum transmitted probe intensity (figure 4). For high modulation frequencies ( $f = 400$ Hz,  $\tau_{\text{pump}} \sim 1.25$ ms  $\sim \tau_T$ ) the effect is no longer dominant, leading to a decrease of the transmitted probe signal and amplitude of modulation. In conclusion, optical nonlinear switching and bistability due to increasing absorption has been observed at room temperature in SDG. Large light by light modulation (10070) was also detected for low modulation frequencies and high pump power. Laser induced clearing and clarkening were detected. Results on dephasing between pump and probe and bistability show that increasing absorption is the dominant effect for low and intermediate pump powers and saturated pump absorption plays an important role in the high pump power regime.

The properties described here show the potential of SDG for nonlinear optical switching and transmission at room temperatures with 100% induced modulation using frequencies up to few KHz.

### Acknowledgements

I would like to thank FINEP and CAPES (Brazilian Agencies) for the financial support.

### References

1. See for example: Proc. of the International Conference on Optical Nonlinearity and Bistability of Semiconductors Berlin, GDR in publ. Phys. Status Solidi 150, 2 (1988).

2. R. K. Jain and R. C. Lind, *J. Opt. Soc. Am.* **73**, 647 (1983).
3. H. Gibbs, *Optical Bistability, Controlling light with light* (Academic Press, Florida., 1985).
4. P. Roussignol, D. Ricard, K. C. Rustagi, and C. Flytzanis, *Opt. Commun.* **55**, 1-13 (1985).
5. P. Roussignol, D. Ricard, J. Lukasik and C. Flytzanis, *J. Opt. Soc. Am.* **B4**, 5 (1987).
6. A. S. B. Sombra, *Opt. and Quantum Electron.* **22**, 335 (1990).
7. A. S. R. Sombra, *Solid State Commun.* **82**, 805 (1992).
8. S. I. M. Haddad, M. Kretzschmar, H. Rossman and F. Henneberger, *Phys. Status Solidi (b)* **138**, 235 (1986); J. Hajto and I. Janossy, *Philos. Mag.*, **47**, 347 (1983).
9. H. M. Gibbs, G. R. Olbright, N. Peyghambarian, H. E. Schmidt, S. W. Koch and H. Haug, *Phys. Rev. A* **32**, 692 (1985).